Chapter 5

Kinematically possible convective flow entities

5.1 Thermals, bubbles, starting plumes, plumes

Coherent structures are common in fluids. Bird watchers and glider pilots know that convective ascent is often concentrated in *thermals*[a] (Ludlam and Scorer 1953), even in clear air, which can be formalized a bit as *bubbles* (Scorer and Ludlam 1953). Long-lived visible *plumes* over fires and smoke stacks are another longtime visual paradigm of turbulent ascent, amenable to controlled study in laboratory tanks[b]. A *starting plume* (Turner 1962) is the combined concept: the response to a localized buoyancy source that is initiated and then maintained. A thorough history and discussion is in chapter 7 of Houze (2014).

Besides observation (indoors and out) and description, thinkers before the computation age had only mathematical study of the fluid dynamical PDEs to fall back on for defining quantitative frameworks. One long-known analytic solution, specific but necessarily idealized, was the vortex ring or spherical vortex (Reynolds 1876, Levine 1959). I have once or twice seen such entities in the sky[c], but they require rare initial and boundary conditions (like skilled lips to blow smoke rings). Still, they can serve as a paradigm for more realistic and ragged entities, a framework for statistical composites of data from turbulent simulations

[a] Glossary of Meteorology: "A discrete buoyant element…small-scale rising current…"

[b] along with less-relevant vertical *jets* driven by initial momentum rather than buoyancy

[c] like the "horseshoe vortex" photo in Fig. 8.28 of Markowski and Richardson (2011).

for instance (like the fruitful debate between Sherwood et al. 2013 and Romps and Charn 2015).

A second equation-based approach is very different, based on concepts of *similarity* or *self-similarity* and depending only on the scale-independent properties of the fluid set (see problem 3.9.4). An admirable high culture in fluid dynamics prizes formal agnosticism equal to our ignorance. Often this is expressed in purely units-based reasoning, or the assertion that flow can only depend on fundamental *nondimensional parameters*[d]. This approach leads to deceptively simple final formulas, like the empirical result that the geometric slope of conical-shaped turbulent plumes is about 0.2 on average (Morton et al. 1956). Lacking any physical scale, such a number is expected to generalize directly from 1m deep water tanks to 1km deep air layers. Although this conical flow is clearly realizable over its layer of similarity, it is not a complete and closed mass circulation, so elaboration is needed near its top (like the starting plume concept). Synthesizing the overly-idealized bubble and incomplete plume entities into mathematical models for use at larger scales (Part III) is a craft as much as a science. One opinionated review of the historical literature and the rather blurry *ad hoc* synthesis in use today is Yano (2014).

One more equation-based approach should be mentioned: the *two-fluid* approach, in which the total flow (satisfying mass continuity) is split into two 'flavors' of air, for instance cloudy and clear (Thuburn group 201x). Bookkeeping equations for the two categories can be written from the pure logic of accounting stuff in space (chapter 1), with terms reflecting the motion of the boundary of these labeled flavors of air as well as the motion of air across that moving boundary -- in whatever manner that boundary may be defined. While fully rigorous, this is really just another accounting tool, and its utility depends entirely on how it is deployed. Its applications are beyond our current scope.

---

[d] https://en.wikipedia.org/wiki/Buckingham_pi_theorem

Might the time average of a sequence of bubbles act like a plume? Most recently, this sequence or chain of bubbles is called a "thermal chain" by Peters et al. 2019. Below a rising bubble, air from the turbulent *wake* below the rising bubble is inexorably drawn up into the core: it turns itself inside out as it rises roughly 3.14 times its radius (Raymond and Lopez 200x). It is better for the entity's longevity if that wake air is buoyancy-enriched, either by a continuing *b* source like in a starting plume, or by air mixtures left behind from an earlier *shedding* or *erosion* process on the sheared and turbulent outer flanks of the bubble itself. Another possibility is enhancement by the dead bodies of prior bubbles that have stalled and mixed out, but enriched the area in ingredients for future bubble buoyancy, like moisture haloes (Rangno and Hobbs 19xx).

The above "better for the entity" statement is the first of many natural-selection arguments we will invoke (as in section 0.5, but note section 0.6's cautions). The spatial coherence of multi-bubble convective *cells,* and of *multi-cellular* aggregate entities, is important to convection's survival and success at doing its job, whatever the details of our conceptualized elementary structure. While research on simple entities continues today, and some essential aspects are important to appreciation and later reasoning, the problem of entity-combination is so crucial that it sets a limit on how fussy it is sensible to get about precision in these elemental realms.

5.1.1 Size and geometry effects on vertical acceleration

Understanding the rising of "parcels" in terms of buoyancy b alone (chapter 4) is incomplete. Realizable ascent of finite-sized fluid elements importantly involves pressure drag. That can be understood as *pressure acting to enforce of the law of mass continuity* by pushing the air above a buoyant element out of the way, and filling the space below as it ascends. In the bargain, *p* opposes the buoyancy force, a tax on the kinetic energy source [*w'b'*] (problem solution 1.5.1) that is redistributed to air displaced in the process. This inertia of the rest of a realizable circulation is sometimes treated as a "virtual mass" factor of about 3, reducing acceleration in the too-simple view *dw/dt = b*.

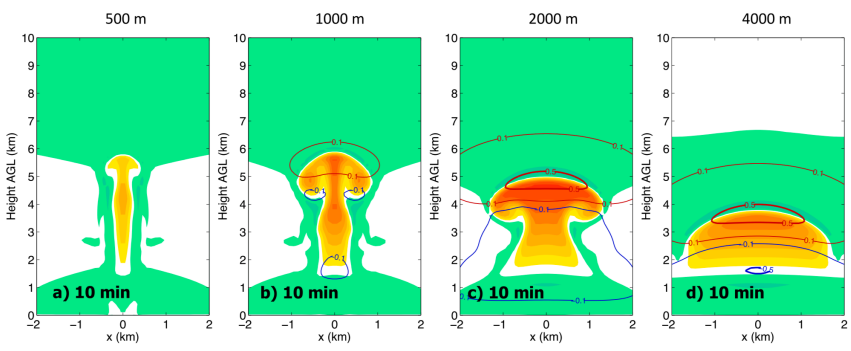

Fig. 5.1. Buoyancy (warm colors for positive values) and π_{buoy} from Eq. (5.1), ten minutes after releasing a bubbles in quiescent air. Narrower drafts feel less opposition from the BPGF, and have ascended further. Fig. 5 of Morrison and Peters (2018).

Pressure's pushback on convective elements can be quantified with our grasping equation for π (problem 1.4.3), revising its conceptual forcing *div*(**F**) for the completed equation set (2.10) in the Boussinesq case as:

$$\begin{aligned} \pi = \ & \boldsymbol{\nabla^{-2}}[b_{\boldsymbol{z}} - \boldsymbol{\nabla} \cdot [(\boldsymbol{V} \cdot \boldsymbol{\nabla})\boldsymbol{V}] + \boldsymbol{\nabla} \cdot \boldsymbol{F}_{Cor}] \\ & = \ \pi_{buoy} \quad + \pi_{dyn} \quad + \pi_{Cor} \end{aligned} \tag{5.1}$$

The $\boldsymbol{\nabla^{-2}}$ operator is linear (allowing the second line's clean decomposition). However, it is *nonlocal* and *scale-selective,* bringing in spatial geometry considerations we can no longer ignore. Evaluating $\boldsymbol{\nabla^{-2}}$ involves two anti-derivatives, requiring constants of integration and/or boundary conditions, so it is just a symbolic thing to write. Pseudo-code for a simple computational approach on a periodic domain (computer exercise 5.5.1) uses the multi-dimensional Fast Fourier Transform **fft** and its inverse **ifft**, with total wavenumber $k_{tot} = [k^2 + l^2 + m^2]^{1/2}$ for spatial wavenumbers *k,l,m:*

$$\pi_{buoy} = \boldsymbol{\nabla^{-2}}(b_{\boldsymbol{z}}) = \mathbf{ifft}[\ {k_{tot}}^{-2}\ \mathbf{fft}(b_{\boldsymbol{z}})] \tag{5.2}$$

Figure 5.2 shows a toy two-dimensional calculation using (5.2) of the net vertical force *b + BPGF,* where BPGF is the vertical force per unit mass $-\partial_z \pi_{buoy}$, for a hypothetical bumpy but uniformly buoyant body (yellow contours over a periodically repeated cloud photo we used to define the bumpy shape).

The feature shape and size dependence of the $\boldsymbol{\nabla^{-2}}$ operation makes the combined vertical force maximize in the growing tips of the tops (brightest reds in lower panel), with the gaps feeling a downward force that acts to enlarge the lobes (pure BPGF since b=0 is assumed there).

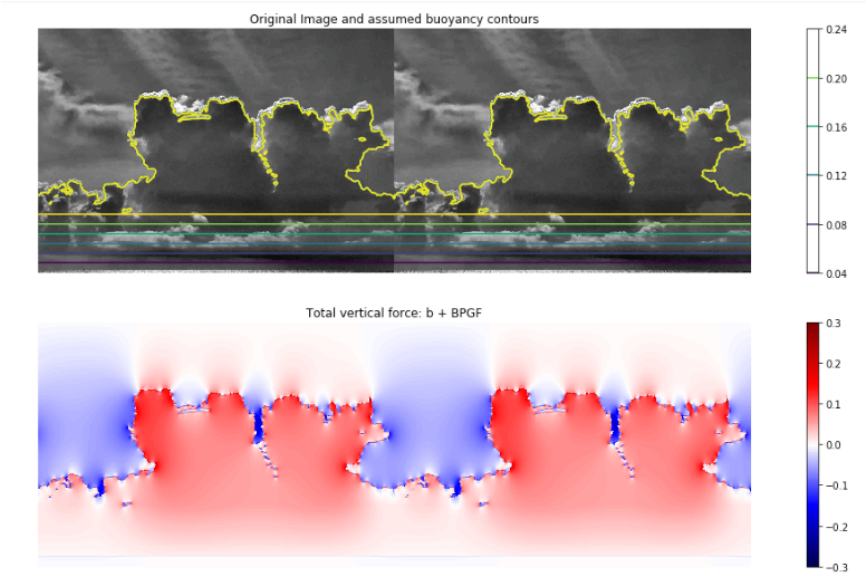

Fig. 5.2. Top: buoyancy (contours), assumed constant and positive in the main cumulus cloud bodies of the underlying photograph). Bottom: Resulting net vertical force b+$BPGF$ computed from π_{buoy} evaluated by Eq. (5.2) for this two-dimensional periodic scene. Units are $m\ s^{-2}$ but values are arbitrary for this linear problem.

The distinctive texture of growing cumulus tops reflects a vital trade-off between opposition to b by the BPGF, which favors narrower entities (Figs. 5.1, 5.2), and vulnerability to mixing which disfavors too-narrow updrafts through thermodynamic destruction of b and viscous 'friction'. Inside even a single cumulus cloud, myriad entities are competing under these influences (along with nonlinear advection and dynamic pressure effects) to create the characteristic cumulus fractal shape with bumps upon bumps. Might this visual texture contain underutilized quantitative information for our science? Many an outdoors person has made better life and death decisions based on a reading of cumulus top textures.

Dynamic pressure is a puzzle, but some insight can be gained. A decomposition from the Boussinesq equations (confirm problem 5.5.2) has a positive definite squared-deformation "splat" term, plus a negative definite squared-vorticity "spin" term:

$$\pi_{dyn} = -\boldsymbol{\nabla^{-2}}(\boldsymbol{def^2} - \boldsymbol{vor^2/2}) \qquad (5.2)$$

(2.131 of Markowski and Richardson 2011), with vorticity $\boldsymbol{vor} = |\boldsymbol{\nabla} \times \boldsymbol{V}|$ and $\boldsymbol{def}^2$ given in summation notation for Cartesian coordinates by

$$\frac{1}{4}\sum_{i=1}^{3}\sum_{j=1}^{3}\left(\frac{\partial u_i}{\partial x_j} + \frac{\partial u_j}{\partial x_i}\right)^2$$

The sense of (5.2) is that *vortices of any rotation direction tend to have lowered pressure* in them, to do the job of holding parcels together against the divergent centrifugal force, while *colliding flows in any direction tens to have elevated pressure*, to push back against the convergent "force" of inertia.

Unfortunately, the common case of straight shear flow has equal but opposite contributions by ***vor*** and ***def***, elementary kinematics tells us, even though it has no actual "spin" or "collision" aspects. This cancellation makes the decomposition (5.2) unsatisfying in realistic complex flows. Perhaps *curvature vorticity* could be isolated usefully with further manipulation, as a way to set aside a residual shear vorticity that is spin-splat balanced, thereby defining some purer 'splat' term in the bargain? The possibility of satisfying causality arguments within the rigorous but slippery mathematics of fluid equations with sound waves filtered out would be greatly desirable.

Another understandable dynamic pressure contribution can be isolated as the interaction of a complex flow entity with a simple mean flow it is supersposed upon. For instance π_{dyn} can explain how a sheared wind impinging on a thermal retards its ascent and creates upshear-downshear asymmetry (Peters et al. 2019), or why right-moving storms are favored by curved wind shear hodographs in splitting supercells (section 8.4 of Markowski and Richardson 2011).

These non-*b* terms in *dw/dt* can be *parameterized* for an isolated updraft entity, based on bubble shape or other assumptions, with uncertain

coefficients estimated by controlled numerical simulations (de Roode et al. 2012, Morrison and Peters 2018, Tian et al. 2019). The lengths to which this kind of frontal assault can be carried are amusingly illustrated by the complexity of Eq. (33) of Morrison (2017):

$$w = \left[\frac{2\mathrm{CAPE}([1/z^2 - 9L_v g k^2 L\Phi/(4c_p P_r R_{\mathrm{HMB}}^2 \mathrm{CAPE})]\{4P_r R_{\mathrm{HMB}}^2 z/(9k^2 L) - 16P_r^2 R_{\mathrm{HMB}}^4/(81k^4 L^2)\ln[9k^2 Lz/(4P_r R_{\mathrm{HMB}}^2) + 1]\})}{1 + \alpha^2 R_{\mathrm{HMB}}^2/H^2 + 3k^2 Lz/R_{\mathrm{HMB}}^2} \right]^{1/2}. \tag{33}$$

We can recognize $w = [2CAPE]^{1/2}$ as the conversion of potential energy (CAPE) to kinetic energy ($w^2/2$) for an inviscid undiluted parcel, which certainly needed some correctives for realizability. But the detail level shades into absurdity if the isolated updraft 'entity' is itself a great idealization. Still, such a formal dependences on radius R could be the seed of a basis for assessing the competition among bubbles of different sizes, a simplest ecology (blind competition among independent entities).

5.2 Downdrafts: condensation-evaporation asymmetry

Negatively buoyant downdraft entities can be envisioned as analogous to buoyant updrafts (bubbles, plumes, etc.) One modern phenomenon of downward moist convection is common in jet condensation trails (Fig. 5.3), evocative of a linear instability theory (periodic, smooth).

Fig. 5.3. Contrail with gentle (periodic, smooth) downward convection of the cloudy air.

Mammatus clouds (darlings of online image and video materials, or search for *asperatus* for even prettier ones) showed this processes before the jet age, an upside-down expression of potential instability (section 0.4) in mean descent of a layer containing cloudy-above-clear sublayers (Ludlam and Scorer 1953, review in Schultz et al. 2006).

While these examples may be nearly moist adiabatic, a few oddities of evaporation in air + condensate mixtures must be recalled from section 2.3.

Buoyancy reversal after the mixing of clear and unsaturated air is peculiar to cloudy convection. The fractional mixture that is just saturated (evaporating all the available condensate) has the greatest bulk density of all possible mixtures. However, this density increase occurs only after complete molecular-scale equilibrium is reached. Turbulent folding (like the *dynamic entrainment* of wake ingestion into a rising bubble discussed above) is not yet mixing, nor is *turbulent entrainment* by shear instabilities on the flanks of narrow updrafts, although that process may lead more quickly to true mixing.

What is the fate of the extra-dense air created by buoyancy reversal? Squires (1958) predicted that it would perforate cumulus clouds with penetrative downdrafts from the mixing at cloud top, while Jonker et al. (2008) emphasize a sheet of descent along cloud edge -- contributing more shear whose instability could drive further mixing. Further discussion of mixing conceptual models and the subsequent sorting of mixtures is in section 6.3.

5.3 2D entities: slabs, jumps, squalls

Entity models of 2D convection in steady state have been devised, featuring “jump” updrafts and “overturning” flow branches that satisfy mass continuity and other Lagrangian (d/dt) conservation laws along trajectories, which are the same as streamlines for steady flow (Moncrieff 1978, 2006). These have become paradigms or "archetypes" for squall momentum flux, but the virtue of their rigor as solutions to the dynamical equations is nontrivial to weave into larger-scale flows, since the far-field asymptote of the flow implies (or requires) a pressure difference across the line that extends out to infinity.

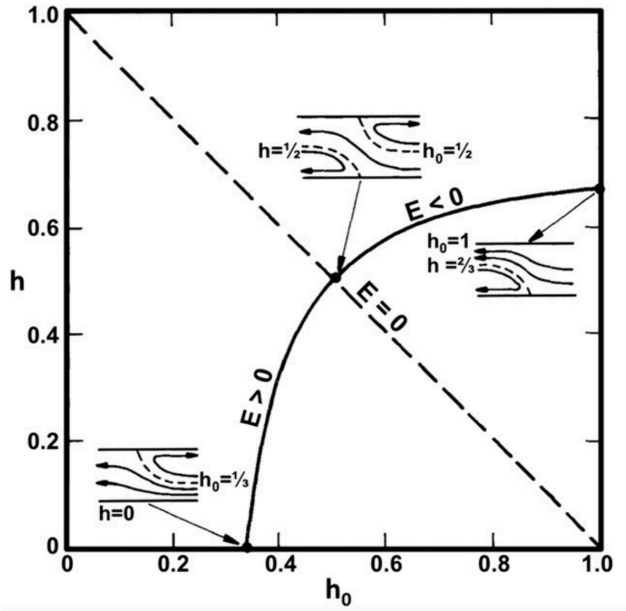

Fig. 5.4. Regime diagram for 2D steady jump and overturning flows bases in rear and front inflow altitudes. Adapted from Fig. 13 of Moncrieff and Lane (2015) where E is defined as a "Bernoulli number" measuring the net pressure drop across the system.

The lack of more and better semi-quantitative models for mesoscale convection, in which the 'dynamic entrainment' implied by the out-of-cloud flow is reconciled with the main updraft's buoyancy flux [$\overline{w'b'}$] required for the system to be energy-generating, remains a major limitation of in atmospheric convection theory. Descriptive models and partial considerations must be stitched together in *ad hoc* ways whose weaknesses remain an Achilles' heel of larger-scale atmospheric dynamics and climate science.

5.4 Problems and exercises

5.4.1 *Dynamic pressure derivation*

Derive Eq. (5.2). Using subscript notation for differentiation will save you many redundant hand motions. Do other decompositions suggest themselves?

5.4.2 *Jupyter notebook on inverse Laplacian*

Reproduce Fig. 5.2 from the Jupyter notebook at github.com/brianmapes/ConvectionShortCourse/BPGF.ipynb. Construct other 2D buoyancy patterns and solve for the implied π_{buoy} and associated BPGF.

5.4.3 *Coalescence and repulsion of buoyant updrafts in 2D*

Explore the effects of a non-random dispatcher function by experimenting with the release times of 3 bubbles of thermal buoyancy b in a convective event in unstratified fluid. The Jupyter notebook at github.com/brianmapes/ConvectionShortCourse/ThreeBubbles.ipynb contains instructions. Optional: relate your work to early model work on multi-bubble clumping and mergers (Wilkins et al. 1976, Orville et al. 1980).

Orville, Harold D., Y.-H. Kuo, R. D. Farley, and C. S. Hwang (1980). Numerical simulation of cloud interactions. *J. Rech. Atmos.* **14**, 499-516.

Wilkins, E. M., Y. K. Sasaki, G. E. Gerber, and W. H. Chaplin, Jr. (1976). Numerical simulation of the lateral interactions between buoyant clouds. *J. Atmos. Sci.* **33**, 1321-1329.

5.4.4 *IDV exploration of Giga-LES data*

Explore the 3D spatial patterns of spatial-eddy temperature (proportional to thermal buoyancy b), perturbation pressure, and other fields in three time steps (5 minutes apart) from a very large and high resolution (giga-

LES) doubly-periodic deep convection simulation. *Capture images that illustrate the relationship between perturbation pressure and terms in (5.2), as best you can find them by focusing on regions where a single term likely dominates.*

Model details are as described at Khairoutdinov et al. (2009), but here the model was forced with domain-mean winds derived from the TWP-ICE program on Jan 20, 2006 over northern Australia (Glenn and Krueger 2017), leading to a ragged south-to-north propagating squall comprising several arc-like segments with more 3D structure. Use Unidata's free IDV software, on a computer with at least 8GB of available RAM (Before attempting this, set the IDV's memory allocation in Edit→Preferences menu, System tab, then restart the IDV.) Instructions and orienting images of the basic fields displays are at github.com/brianmapes/ConvectionShortCourse/GigaLES.ipynb.